

**NISTIR 89-4030**



# **Ignition and Lateral Flame Spread Characteristics of Certain Composite Materials**

T. Ohlemiller  
S. Dolan

U.S. DEPARTMENT OF COMMERCE  
National Institute of Standards and Technology  
(Formerly National Bureau of Standards)  
National Engineering Laboratory  
Center for Fire Research  
Gaithersburg, MD 20899

January 1989

Sponsored by:  
David Taylor Research Center  
United States Navy  
Annapolis, MD



**NISTIR 89-4030**

# **Ignition and Lateral Flame Spread Characteristics of Certain Composite Materials**

T. Ohlemiller  
S. Dolan

U.S. DEPARTMENT OF COMMERCE  
National Institute of Standards and Technology  
(Formerly National Bureau of Standards)  
National Engineering Laboratory  
Center for Fire Research  
Gaithersburg, MD 20899

January 1989



National Bureau of Standards became the National Institute of Standards and Technology on August 23, 1988, when the Omnibus Trade and Competitiveness Act was signed. NIST retains all NBS functions. Its new programs will encourage improved use of technology by U.S. industry.

Sponsored by:  
David Taylor Research Center  
United States Navy  
Annapolis, MD

**U.S. DEPARTMENT OF COMMERCE**  
**C. William Verity, Secretary**  
**Ernest Ambler, Acting Undersecretary**  
**for Technology**  
**NATIONAL INSTITUTE OF STANDARDS**  
**AND TECHNOLOGY**  
**Raymond G. Kammer, Acting Director**



## TABLE OF CONTENTS

	<u>Page</u>
List of Tables . . . . .	iv
List of Figures . . . . .	v
Abstract . . . . .	1
1. Introduction . . . . .	1
2. Experimental . . . . .	2
Materials . . . . .	2
Measurement Techniques . . . . .	3
3. Results and Discussion . . . . .	4
3.1. Ignitability . . . . .	4
Sample Behavior . . . . .	4
Heat Flux Dependence of Ignition Delay . . . . .	5
Correlation of Ignition Data . . . . .	6
3.2. Lateral Flame Spread . . . . .	8
Sample Behavior . . . . .	8
Lateral Flame Spread Parameters. . . . .	9
4. Summary and Conclusions . . . . .	11
5. References . . . . .	13

LIST OF TABLES

	<u>Page</u>
Table 1. Parameters Inferred from LIFT Ignition Data . . . . .	14
Table 2. Parameters Inferred from LIFT Flame Spread Data . . . . .	14

## LIST OF FIGURES

		<u>Page</u>
Figure 1.	Ignition delay time vs. incident heat flux for CG Camel honeycomb panel. Equation shown is least-squares fit and R is the correlation coefficient. . . . .	15
Figure 2.	Ignition delay vs. incident heat flux for CG Camel and CG Yellow honeycomb panels . . . . .	15
Figure 3.	Ignition delay time vs. incident heat flux for CG Yellow honeycomb panel; face and edge ignition data points are distinguished . . . . .	16
Figure 4.	Ignition delay time vs. incident heat flux for CG Green Vinyl honeycomb panel. Equation shown is least-squares fit and R is the correlation coefficient . . . . .	16
Figure 5.	Ignition delay time vs. incident heat flux for OC Armor composite armor panel. Face and edge data points are distinguished. Equations shown are least-squares fits and R values are correlation coefficients . . . . .	17
Figure 6.	Ignition model correlation for CG Camel and CG Yellow treated as a single material. Data points for face ignition only. . . . .	18
Figure 7.	Ignition model correlation for CG Green Vinyl. Data points for face ignition only . . . . .	18
Figure 8.	Ignition model correlation for face ignition of OC Armor . . . . .	19
Figure 9.	Ignition model correlation for edge ignition of OC Armor . . . . .	19
Figure 10.	Experimental data for lateral flame spread on OC Armor. Edge and face data are distinguished. The value of $q_e$ is the peak incident flux on the sample face . . . . .	20
Figure 11.	Experimental data for lateral flame spread on CG Camel honeycomb panel. Data shown are for sample edges. Each test was run at a different value of the peak incident heat flux, $q_e$ . . . . .	20

Figure 12. Experimental data for lateral flame spread on CG Camel honeycomb panel. Data are for sample face. Results for two different values of the peak incident heat flux are shown. . . . . 21

Figure 13. Model correlation of lateral flame spread on CG Green Vinyl honeycomb panel. Line shown has been forced to pass through a value of  $0.87 \text{ W/cm}^2$  on the horizontal axis . . . . . 21

Figure 14. Distribution of heat flux incident on sample surface, normalized by peak value . . . . . 22

# Ignition and Lateral Flame Spread Characteristics of Certain Composite Materials

## Abstract

The LIFT apparatus was used to obtain information on the ignition and lateral flame spread characteristics of two types of composite materials. The first type was a honeycomb sandwich panel; three different facings were tested with this material. The second type of material was a composite armor. There was a substantial variation in the ignitability of the various material combinations with a vinyl-faced honeycomb panel being the most ignitable and the composite armor being the least ignitable. The ignition behavior of the facings of all materials was correlated by a simple predictive model. Only the vinyl-faced honeycomb panel showed significant normal flame spread under the conditions examined though some flame "advancement" was seen with the others. All of the materials exhibited worse flammability properties at their edges as compared to their facings.

## 1) Introduction

This report summarizes the results of ignitability and lateral flame spread tests performed on two substantially different types of composite materials, Nomex sandwich panels and a composite ballistic armor. The tests were performed using the Lateral Ignition and Flame Spread (LIFT) apparatus at the NIST Center for Fire Research. The objective is to begin to establish a database on the flammability of materials of potential interest to the Navy for shipboard applications such as the Composite Deckhouse.

The general approach to flammability assessment followed here is discussed in detail in Reference 1. Briefly, the approach consists of determining sets of effective parameter values which can be utilized in the context of simplified models of ignition or flame spread to predict this behavior in a variety of different contexts. Examples of such parameters are the minimum surface temperature for ignition and the minimum incident heat flux on a material surface necessary to support continued flame spread.

The principal measure of ignitability is the delay time between the onset of a constant heat flux to the surface of a material and the first appearance of a flammable mixture of gases issuing from the surface of the material. The presence of a flammable gas mixture is sensed by placing a small pilot flame in the gas stream issuing from the surface (positioned so that it does not add to the external heat flux on the sample surface). The delay time is dependent on the incident flux level; a complete ignitability characterization thus uses a range of heat fluxes from 7 or 8 W/cm<sup>2</sup> down to the minimum flux necessary for ignition. This minimum is dependent on the physical and chemical characteristics of the material as well as the conditions of heat exposure. These measured data are fitted to a simple model of the ignition process to

infer the values of two parameters in the model: the effective thermal inertia of the sample (product of thermal conductivity, density and heat capacity) and the minimum surface temperature for ignition. The model equation can then be used to predict the ignition delay for the sample material in other conditions such as for larger scale vertical surfaces.

Flame spread rates on vertical flat surfaces are approximately equal in both the lateral and downward directions; spread rates on horizontal flat surfaces are also comparable [2, 3]. Thus only one of these configurations (all of which involve opposed flow flame spread; see Ref. 1) needs to be measured to obtain the expected behavior for all three. The LIFT apparatus measures lateral spread on a vertical surface. This rate is dependent on the temperature of the surface ahead of the spreading flame. This temperature could be increased in a fire by an external heat flux (from some other burning object, for example) incident for a varying amount of time. Generally such an external flux can increase the sample surface temperature only up to an equilibrium value dependent on that flux level and on the rate of heat loss from the surface. The LIFT apparatus takes this preheating effect into account by first allowing the sample surface to equilibrate locally with an external flux. This local flux varies monotonically along the surface of the sample so that one can obtain a measure of the heat flux dependence of the lateral flame spread velocity. Furthermore, one can obtain the minimum flux at which sustained lateral spread is possible. By fitting these data to a simplified model of opposed flow flame spread, one can obtain another effective parameter for the material, a measure of the flame heat transfer to the sample surface during flame spread. The fitted model can then be used to predict the opposed flow flame spread rate of the material in any of the configurations mentioned above for larger-sized samples.

These are the procedures applied to the materials of interest here. They met with varying degrees of success due to peculiarities of sample behavior, as discussed below.

## 2) Experimental

Materials: All samples were obtained from the U. S. Navy David Taylor Research Center; they are the first in a series of composite materials to be subjected to an extensive flammability characterization in aid of their evaluation for shipboard use. The first type of composite was a Nomex honeycomb sandwich panel<sup>1</sup>. Three different panels were tested having different finishes on the heated surface. Two of the finishes appeared to be substantially similar, differing only in color. One was described as "camel" in color; the other was yellow. For both of these the color layer had the appearance of a low gloss paint intimately bonded to the layers below. The third surface finish on the honeycomb panels was apparently a textured vinyl sheet, light green-yellow in color, that appeared to be glued to the outermost

---

<sup>1</sup>Product names are provided here only for purposes of clarity; they do not imply any endorsement by NIST.

layer of the sandwich panel; this vinyl layer was readily strippable from the sandwich panel. All of these panels were nominally 15 ½ mm (5/8 in.) thick and the honeycomb core accounted for approximately 8 mm (1/2 in.) of this thickness. The sandwich faces were multilayer in character including one or more plies of woven glass fibers. In the results that follow, these panels are designated as CG Camel, CG Yellow and CG Green Vinyl.

The second type of material was a composite armor based on S-2 glass and a phenolic resin; this was a ballistic armor designed for stopping the penetration of small, high speed metal fragments. The glass is in the form of a large number of woven roving plies with the resin dispersed throughout. The high glass content (80 % by weight) necessitated that this material be cut to size for the tests by means of a diamond saw. The nominal thickness was 12 ½ mm (1/2 in.). In the results below this material is designated as OC Armor.

Measurement Techniques: The LIFT apparatus was used for both the ignitability and lateral flame spread measurements. For the ignition tests the sample was 156 mm (6 1/8 in.) square and it was placed in the end of the LIFT sample holder which provides a nearly uniform heat flux from a gas-fired panel. The procedures followed with regard to calibration and test measurements were those currently under consideration by ASTM [4]. Briefly, a dummy specimen, fabricated to support a heat flux gage, is mounted in the apparatus. The radiant panel and the pilot flame (acetylene / air), positioned above the top edge of the sample, are stabilized and the flux to the specimen surface is recorded. The dummy specimen holder is quickly removed and the actual specimen holder rapidly inserted. At full insertion a stopwatch is started. The test ends when a flame is attached somewhere on the sample and the requisite time for this is noted from the stopwatch. Flame attachment means that a gas phase flame has its base on the sample so that its own heat flux assures a continuing flow of fuel gases from the sample to feed the flame. It is not necessary that the foot of the flame cover a large portion of the sample face or the sample edge to satisfy this criterion and, in fact, it frequently did not. Prior to flame attachment, flashes of flame were often seen; these would propagate rapidly from the pilot flame to some region of the sample surface and then disappear. Such a phenomenon does not represent true ignition. These procedures were repeated with new samples at several heat flux levels to establish the variation of ignition delay time with heat flux. Establishment of the minimum heat flux for ignition generally requires several tests in which one attempts to bracket the limit. The longest delay time one waits for ignition has been arbitrarily set at 22 minutes. It is apparent from the resulting data that this is adequate.

The lateral flame spread tests were run in the same apparatus but with longer samples (794 mm or 31 ½ in.). As noted above, the sample temperature affects the flame spread rate. The normal procedure calls for pre-heating the sample until it reaches equilibrium with the local incident flux (recall this varies along the length of the sample). This procedure was followed except in the case of the CG Green Vinyl material. Waiting for full thermal equilibrium here allowed the vinyl surface coating to fully degrade to the point where it was not ignitable by the usual ignition method. The length of time required for thermal equilibrium with the incident heat flux is determined from the

ignitability results by correlating them in a manner which is illustrated below. After pre-heating (typically with the maximum flux just above the minimum for ignition) the gases issuing from the surface are ignited with a pilot flame and flame spread on the pre-heated surface is initiated. Progress of the flame front across the sample face (toward the direction of lower incident heat flux) is followed visually with an optical arrangement which allows determination of the times at which the flame reaches pre-determined positions (typically 25 mm apart). The flame front is not necessarily flat; one normally focuses on the progress of the flame across the mid-height of the sample. The actual flux incident at each position is precisely calibrated beforehand. Thus when the flame reaches a position on the sample face beyond which it will not propagate, one knows the corresponding minimum heat flux for lateral flame spread (and the corresponding minimum sample surface temperature for continued spread). This same procedure is repeated for three separate samples of each material.

### 3) Results and Discussion

#### 3.1) Ignitability

Sample Behavior. All of the samples exhibited some form of idiosyncratic behavior when heated. CG Camel and CG Yellow behaved alike. Both underwent an explosive delamination of the outermost layers relatively early in the heating process. This appeared to be due to the volatility of some component binding these layers together; when it began to vaporize, the vapors could not escape through the non-porous "paint" layer. Bubbles formed between layers, expanded and then blew loose all layers down to the outermost glass ply. Sometimes these bubbles turned the sample face into an irregular surface with several "flaps" of loosened material opening out randomly; other times most of the sample surface was occupied by one large "flap" of disrupted material. In all cases these flaps undoubtedly sharply altered the flow of heat into the sample interior. Soon after the explosive delamination the various protruding fragments of the outer layers charred rapidly with a considerable efflux of white smoke. Only at high incident fluxes did this smoke ignite and only then did the actual face of the sample ignite. When a sample was exposed to lower fluxes this smoke emission ended and many minutes passed before visually smaller amounts of smoke began to be emitted once again. In the interim the glass plies detached from the Nomex core, also as a result of internal pressure, but they remained intact, merely bulging outward about 1/2 cm in the sample center; this too must have affected the heat flow in the sample. This internal pressure was evidently relieved out through the edge of the sample; this appeared to establish a pathway to the outside used preferentially by all subsequent gases generated in the sample interior. As a consequence, the ignition and subsequent burning of the sample at these lower fluxes was at one or more edges exclusively.

The CG Green Vinyl samples might potentially have behaved in a similar manner since it appears to have a structure similar to the other CG materials. However, the surface layer of (presumed) vinyl material was so much more flammable than the surface layers of the other two CG materials that it dominated the observed behavior. This layer rapidly softened and bubbled,

even at very low fluxes. The bubbles swelled considerably, sagged and charred with emission of visible smoke. The bubbles, some of which were several centimeters in diameter, undoubtedly have a substantial effect on the heat transfer in the sample. The evolved smoke was readily ignited by the pilot flame with subsequent flaming over most of the sample face. The burning of this vinyl facing lasted long enough (up to two minutes) for it to be considered the primary hazard. The subsequent ignition and burning of the deeper layers of the composite, analogous to the behavior noted for the other two CG materials, was noted in a few tests but was not followed in detail.

The OC Armor, with its drastically different structure, behaved quite differently from the above materials in some respects. The geometry of the material never changed at any time in an ignition test. The surface simply turned black slowly with very little visible smoke emission. The high mass per unit of facial area of the material slowed the heat-up and subsequent ignition process. Flaming ignition, when it finally occurred, was either at the sample edge or at the sample face. Face ignition was always localized to one or a few very small (few mm) jets of gas which appeared to issue from pinpoint defects in the sample face. Typically, as time increased, the size of each flame increased somewhat, as did the number of jet-like flames. However, the full facial area of the sample was never involved in flaming. Edge ignition was more diffuse; it presumably resulted from defects which happened to be near the cut edges of the sample. Unlike the situation with the CG samples, here edge ignition or face ignition could occur over the same flux range (see below).

Heat Flux Dependence of Ignition Delay. Figure 1 shows the ignition delay time for CG Camel as a function of the incident radiant heat flux. The line through the data points is a best fit polynomial, not an ignition model line; the model fit is discussed below. Clearly, the incident flux has a drastic effect on the ignition delay time especially as one gets near the minimum flux for ignition (here about  $2.2 \text{ W/cm}^2$ ). What is not apparent from the smooth line in the Figure is that there is a transition in the range from about  $3.0$  to  $4.0 \text{ W/cm}^2$  from edge ignition (at lower fluxes) to face ignition (at higher fluxes).

The implication of this behavior is that edge effects are extending the flux range over which this material will ignite. That is, it appears that in the absence of edge effects, the minimum flux for ignition might be closer to  $3.2$  rather than  $2.2 \text{ W/cm}^2$ . This is only an estimate of the edge effect; we will be pursuing this issue more precisely in the future with a different sample holder which should eliminate edge ignition. It is important to separate out edge effects for two reasons. First, they are real and probably are to be found in full scale fires where they may worsen the flammability of a material, as here. Thus it is important to be able to isolate and study these effects separately. Second, these effects probably will not follow the simplified ignition model used to apply face ignition results from the LIFT apparatus to other situations. There is reason to believe that the edge effects may be scale dependent, in contrast to face ignition behavior. As a result one has to be cautious in using the polynomial fit shown in each of the Figures having ignition data; the polynomial describes the data shown quite

well but it may fail to do so at some larger or smaller scale for the heated sample area.

It was noted above that the physical behavior of the CG Camel and CG Yellow samples was essentially the same. Figure 2 shows that their ignition behavior was indistinguishable within the variability of the samples. Evidently they are virtually identical in composition except for the pigment in the face "paint". The reflectivity of the two surfaces (Camel and Yellow) for infrared radiation from the gas-fired panel in the LIFT apparatus is apparently not significantly different. Figure 3, with an expanded vertical scale, shows the sharp separation, seen with the CG Yellow material, between edge ignition and face ignition.

Figure 4 shows the ignition behavior of CG Green Vinyl; note the expanded vertical scale. The vinyl facing clearly has a deleterious effect on ignitability. The minimum flux for ignition has moved down to about  $1 \text{ W/cm}^2$ . The ignition delay time at  $2 \text{ W/cm}^2$  has gone from something greater than 20 minutes (perhaps infinity) for the CG Camel or CG Yellow down to about 40 seconds.

Figure 5 shows the ignition results for the OC Armor composite; this is the most ignition-resistant material of all those examined here. Note that edge effects once again have extended the flammability of a material; here the minimum flux for face ignition is about  $1 \text{ W/cm}^2$  higher than it is for edge ignition (approx.  $4.5$  vs.  $3.5 \text{ W/cm}^2$ ). Now, however, the edge effects continue throughout the flux range where ignition was observed. This implies that for any given sample at any flux, ignition may occur unpredictably at an edge or on the sample face. Since ignition appears to be a result of gases generated at or preferentially escaping from localized defects in the sample, the ignition site apparently depends on whether weaker defects happen to be on the sample face or near an edge. For this material, in contrast to the CG materials above, edge ignition was not obviously associated with internal delamination creating lower resistance gas flow paths out through the sample edges. However, the fact that edge ignition always occurred more readily than face ignition suggests that gases could more easily escape to the edges when a defect was present near an edge.

Correlation of Ignition Data. As discussed in Ref. 1, the ignition delay time data from a variety of materials can be correlated in a simple manner from which one can infer parameters for the ignition and flame spread models. The ignition model predicts that a plot (through the origin) of  $(q_{ig}/q_e)$  vs the square root of the ignition delay time will give a straight line. Here  $q_{ig}$  is the minimum flux necessary for ignition and  $q_e$  is the incident flux needed to yield a given ignition delay time. The model underlying this relationship is one-dimensional. Thus it does not anticipate the edge effects seen with some of these materials. For this reason we have applied this correlation, for the most part, only to the face ignition data. The results are shown in Figures 6 - 8; the correlation is reasonable in all cases. Note that the CG Camel and CG Yellow materials are treated as one for this purpose in Fig. 6.

The objective in seeking this correlation is the parameter values one can infer from it. The intercept of the correlation line with the unity value of the flux ratio gives one a working measure of the time needed for an externally heated sample of the given material to come to thermal equilibrium with an external flux (regardless of the value of the flux). This value is used as a pre-heat time in the lateral flame spread tests discussed below (with some exceptions as noted below). A second parameter is the effective thermal inertia (product of thermal conductivity, density and heat capacity) of the sample. Since some of the samples undergo drastic physical changes during the ignition process, this parameter is quite empirical, being an average over the changing sample structure. A third parameter is the effective surface temperature of the sample at ignition. This uses a experimental correlation [4] developed for materials whose physical deterioration during ignition was much less than some of that seen here so, again, the result must be viewed as an effective empirical value rather than the real surface temperature (the surface of some of the present materials is not at all well-defined by the time of ignition). With these caveats in mind, the inferred parameter values can be found in Table 1. The thermal inertia and effective ignition temperature are used in the model equation for lateral flame spread rate (see below). The slope in plots such as Figures 6 - 8, denoted here as "b", is used in the following expression for calculating ignition delay times.

$$(q_{ig}/q_e) = \begin{cases} bt^{\frac{1}{2}}, & t \leq t_m \\ 1, & t > t_m \end{cases}$$

Here  $t$  is the ignition delay time and  $t_m$  is the thermal equilibrium time discussed above. Putting the appropriate parameter values from Table 1 into this expression, one finds that it generally gives a fairly accurate prediction of the observed ignition delay times for the sample face, especially for engineering purposes; the accuracy of the predictions is comparable to that seen for the correlation lines in Figures 6 -8. These predictions for face ignition delay time should be adequate for these materials if the heated area is three to four times larger than that used in the LIFT apparatus [1]. Beyond this range some checking should be done.

The same data reduction procedures and correlations can be used for the edge ignition results. Figure 9 shows such a correlation for OC Armor; the correlation looks quite good. In general, however, the edge correlations do not look this good. Furthermore, as noted above, the model used for both ignition and lateral flame spread does not consider such non one-dimensional effects as edge ignition and burning. Again, there is good reason to believe that edge effects are scale dependent. This whole issue needs further study; it appears to be of considerable importance in the flammability of composites which exhibit non-isotropic properties.

### 3.2) Lateral Flame Spread

Sample Behavior. The physical behavior of the samples was in all cases similar to that described above for ignition. The impact of this behavior on flame spread varied with the sample formulation.

The primary data from the flame spread tests are plots of the most forward flame position as a function of time. Examples of these are shown in Figures 10 - 12. On these plots the incident flux varies with position as shown in Figure 14. There one can see that it is fairly constant for the first 150 mm or so; it then decays monotonically in a nearly linear manner. At 500 mm the incident flux is down to about 20% of the peak value.

The slope of the plots in Figures 10 - 12 is the inverse of the spread velocity. Thus the nearly horizontal sets of points in Fig. 11, for example, imply a very high spread rate. Actually flame spread in the normal sense was not seen with most of these samples because of complications in their physical behavior, as discussed below.

CG Camel delaminated the most on the high flux end of the sample, as would be expected. While there was a good deal of flaming, which could last up to 20 minutes subsequent to ignition, there was no real organized flame spread process during this time. An organized flame spread process is one in which heat transfer from the flames in the ignited region of the sample causes a smooth movement of the flame toward regions of the sample that are cooler by virtue of their receiving a lower incident heat flux from the radiant panel. As was noted above, the delamination process left fuel gas exit paths at random locations around the edges of the sample; here these paths led out through the three edges around the high flux end of the sample. Burning of the gas streams emerging from various points along these edges did not lead to smooth propagation of the flames along the edge. The appearance of flame spread along the edges was noted in some cases, i. e., after some time flames did appear at points along the edges which were in the direction of a lower incident radiant flux. However, this was always spatially discontinuous; it seemed to be due to delayed piloted ignition of gas streams that may have been present from the original delamination process. If the delamination process itself was propagating, it was not apparent. Some attempts were made to obtain flame spread on the front face material by using a pre-heat flux high enough to cause face ignition; these samples tended to ignite spontaneously during the attempted pre-heat interval (which was evidently too long) and did not give the desired facial flame spread. The explosive delamination early in the heat-up may preclude this since it breaks the facial material into random, disconnected segments. CG Yellow was not tested for lateral flame spread since it behaved so similarly to CG Camel in the ignition tests.

CG Green Vinyl came closest to exhibiting a simple flame spread process across the sample face. There were two complications. First, as noted above, the vinyl layer swelled with large scale (several cm) bubbles; these made the spread process somewhat erratic. Second, as was also noted above, the vinyl surface layer tended to char and become largely inert if it was subjected to an extended period of pre-heating. For this material, the normal procedure was altered. Instead of pre-heating the sample to its thermal equilibrium

time, it was pre-heated only for the normal ignition delay time for the particular flux chosen. This interval was assured by keeping the acetylene / air pilot flame lit during the pre-heat period; it ignited the evolved gases as soon as they reached a flammable concentration.

OC Armor also did not exhibit an organized flame spread process. As noted above, flaming was always localized to small jets emerging from the sample face or to gases emerging from the sample edges. There was essentially no spread of the edge flames. There was some semblance of spread with the face jets in that newly flaming jets appeared after some time interval in cooler regions of the sample face. The new jets were never contiguous to previous jets, however. Thus they were not the result of localized heat transfer causing a given jet to become larger; they could have been the result of heat transfer through the sample from the total assembly of flaming jets on the sample face.

Lateral Flame Spread Parameters. In light of the above discussion, there is no correlation to be made of the data for any of the materials except CG Green Vinyl because only it appeared to yield a true flame spread process. Before turning to this last material, however, one can estimate lower bounds for a pair of useful parameters for the other materials. These parameters are the minimum incident heat flux necessary to support lateral flame spread and the minimum temperature of the sample surface (ahead of any flame heating effects) necessary to support lateral spread. These two parameters are interrelated; the temperature is that achieved on the sample surface at thermal equilibrium with the minimum incident heat flux. This flux is estimated from the position of the forward-most flames in the LIFT spread tests coupled with the pre-calibrated flux versus position. The results are shown on Table 2;  $q_s$  is the flux incident on the location of most forward flame appearance and  $T_{s, \min}$  is the surface temperature achievable at thermal equilibrium when this flux is incident.

For CG Camel the most forward flames were on the edges at a position corresponding to the flux shown; the large scatter in this flux (from three tests) is a result of the random emergence of the gas streams along the sample edges. The corresponding minimum sample surface temperature for flame spread is shown in parentheses because it is higher than the minimum ignition temperature for this material shown in Table 1. In the context of the simplified model for ignition and lateral flame spread described in Reference 1, this result is contradictory. The highest sample surface temperature allowed is equal to the minimum ignition temperature itself because achieving this temperature in pre-heat would lead to an infinite flame spread rate upon ignition (ignition everywhere at once). The source of this discrepancy for this material is probably the dominance of edge effects not accounted for in the model (plus scatter in the experimental data<sup>2</sup>).

---

<sup>2</sup> It is not uncommon, even for materials which behave better than those studied here, for the minimum ignition temperature and minimum sample surface temperature for flame spread to appear to be inverted as they do here. Data scatter coupled with simplifications in both the ignition and flame spread models probably account for this.

CG Green Vinyl also shows a discrepancy between the estimate of the minimum pre-heat temperature for flame spread and the ignition temperature of the material in Table 1. This cannot be attributed to edge effects since the behavior under consideration for this material is strictly facial (both ignition and lateral flame spread). Recall that this material was unique in that the full pre-heat time could not be allowed; it caused complete charring of the thin vinyl layer and a subsequent lack of flame spread. It is probably this same phenomenon which halts flame spread (or at least contributes to the halt) since the equilibrium pre-heat time (268 s from Table 1), which causes complete charring of the vinyl, is comparable to the absolute heat flux exposure times at which flame spread stops in some of the tests. This is a reactant depletion effect which is not included in the models of ignition and flame spread used for correlating the data. It is particularly pertinent to thin flammable layers atop a less flammable substrate.

Oc Armor did not exhibit normal lateral flame spread, as discussed above, but the behavior of the minimum pre-heat temperature in Table 2 is at least consistent with the model expectations; it is 45 °C less than the minimum face ignition temperature in Table 1. The flame on the sample edges typically reached slightly greater distances than that on the sample face; the minimum heat flux for the edge flames is thus about 10 - 15% lower than the value shown in Table 2. The high minimum pre-heat temperature and the corresponding high value for the minimum flux for flame spread indicate the relatively high stability of this material. It is relatively difficult to ignite and it resists lateral flame spread.

As noted above, CG Green Vinyl came closest to exhibiting a normal flame spread process though this had to be examined at a lesser than usual extent of pre-heating. For this reason an attempt was made to correlate the spread data in the manner used to obtain a parameter for the flame spread model equation. The model equation is the following:

$$V = \Phi / (k\rho C)(T_{ig} - T_s)^2$$

Here V is the lateral flame spread velocity,  $\Phi$  is the parameter whose value we seek; it is a measure of the heat transferred from the flame to the sample surface ahead of the flame,  $(k\rho C)$  is the thermal inertia of the sample (its value was inferred from the ignition data: see Table 1),  $T_{ig}$  is the sample surface temperature at ignition (again see Table 1) and  $T_s$  is the temperature of the sample ahead of the flame front (likely to be elevated by pre-heating from an external flux; this effect is calculable; Ref. 1). Thus the only unknown in this equation for flame spread velocity is  $\Phi$ . A plot of the flame spread data such as that shown in Figure 13 allows one to infer the value of  $\Phi$ ; it is related to the slope. The data in Fig.13 are problematical in that regard, however. The scatter is such that the true slope is quite hard to discern. The line drawn there was forced to go through the point on the horizontal axis equal to 0.87 W/cm<sup>2</sup>. This is the minimum heat flux for

---

ignition determined for the CG Green Vinyl material (see Table 1); the model says the data should converge on this point. The line in the Figure is plausible but not fully convincing. The value of  $\Phi$  one infers from its slope is 710 in units appropriate for use with the other parameters in Table 1. Using this to predict flame spread velocities as a function of  $T_s$  (and thus as a function of equivalent incident heat fluxes, assuming thermal equilibrium) gives a set of numbers which behave plausibly but which cannot be checked directly since they call for incident fluxes below the minimum for the LIFT apparatus (approximately  $1 \text{ W/cm}_2$ ). Again, there is a phenomenon occurring with this material, reactant depletion, which is not included in the theory which gives rise to the above equation. Thus one cannot expect it to give a perfect correlation of the data or to produce a perfect predictive result. The preceding does illustrate the process whereby one goes from the raw data to a predictive equation; this process has been shown elsewhere [2,5] to yield useful results for a variety of materials, including composites for aircraft interiors.

#### 4) Summary and Conclusions

The two types of composite material tested here were distinctly different in physical structure; the first type was a honeycomb sandwich panel and the second was a high density composite armor. Three different facings were examined on the honeycomb panels. Two apparently differed only in color; the ignitability behavior (ignition delay time versus incident heat flux level) of these two was so similar that separate lateral flame spread tests were deemed unnecessary. The third honeycomb panel had a facing that appeared to be a thin vinyl sheet. This sheet proved to be much more flammable than the underlying panel structure; its ignition delay time at any given flux was less than that of the other two honeycomb panels, as was its minimum incident flux for lateral flame spread. The composite armor material had a higher mass per unit of exposed facial area than the honeycomb panels, potentially providing a greater fuel load, but it also was 80% percent glass by mass. This material was the most ignition resistant of those tested here.

Only the honeycomb panel with the vinyl facing exhibited a simple flame spread process; even this was made erratic by large bubbles and it was also evidently affected by charring of the vinyl ahead of the flame front at long exposure times. The other materials allowed some slight advancement of flames on their heated faces but this was not flame spread in the normal sense. Here again flames progressed the least on the composite armor.

The ignition behavior of these materials was correlated with reasonable success by the simplified ignition model described in Reference 1. An attempt was made to apply the flame spread model described there only to the vinyl-faced honeycomb panel; this was a partial success apparently limited by reactant consumption effects not included in the model.

All of the above materials exhibited greater flammability around the sample edges than on the sample face. In ignition this meant lesser ignition delays on the edges or preferential ignition at the edges in part of the incident

heat flux range. In lateral flame spread this meant that the flames progressed further along the edges than along the face. The edge effects appear to be tied to a tendency for the composite to delaminate and produce preferential paths for gas flow out the edges rather than out through the face even though this latter path may be much shorter. These edge effects deserve much closer study to determine how they vary with sample size and to ascertain to what extent they can be predicted and controlled.

## References

- 1) Ohlemiller, T., "Assessing the Flammability of Composite Materials", National Institute of Standards and Technology Interim Report, in review.
- 2) Quintiere, J., Harkleroad, M. and Walton, D., "Measurement of Material Flame Spread Properties", Combustion Science and Technology 32, (1983), p. 67
- 3) Atreya, A., Carpentier, C. and Harkleroad, M., "Effect of Sample Orientation on Piloted Ignition and Flame Spread", Proceedings of the First IAFSS International Symposium, Hemisphere Publishing Co., New York, (1986), p. 97
- 4) Quintiere, J. and Harkleroad, M., "New Concepts for Measuring Flame Spread Properties", Fire Safety Science and Engineering, ASTM Special Technical Testing Publication 882, Philadelphia, (1985), p. 239
- 5) Harkleroad, M., "Ignition and Flame Spread Measurements of Aircraft Lining Materials", National Bureau of Standards NBSIR 88-3773, May, 1988

Table 1

Parameters Inferred from LIFT Ignition Data\*

<u>Material</u>	$\dot{q}_{ig}$ (W/cm <sup>2</sup> )	$T_{ig}$ (°C)	$b$ (s <sup>-<math>\frac{1}{2}</math></sup> )	$t_m$ (s)	$(k\rho c) \left( \frac{kW}{m^2K} \right)^2 \cdot s$
CG Camel + Yellow	3.50	450	0.100	100	0.88
CG Green Vinyl	0.87	275	0.061	268	0.43
OC Armor	4.70	630	0.033	930	7.20

\*above are for face ignition, not edge ignition

Table 2

Parameters Inferred from LIFT Flame Spread Data

<u>Material</u>	$\dot{q}_s$ (W/cm <sup>2</sup> )	$T_{s,min}$ (°C)
CG Camel <sup>a</sup>	3.1 ± .4	(530)
CG Green Vinyl <sup>b</sup>	1.2 ± .2	(330)
OC Armor <sup>b</sup>	3.8 ± .1	585

<sup>a</sup> edge

<sup>b</sup> face

### CG Camel Ignition

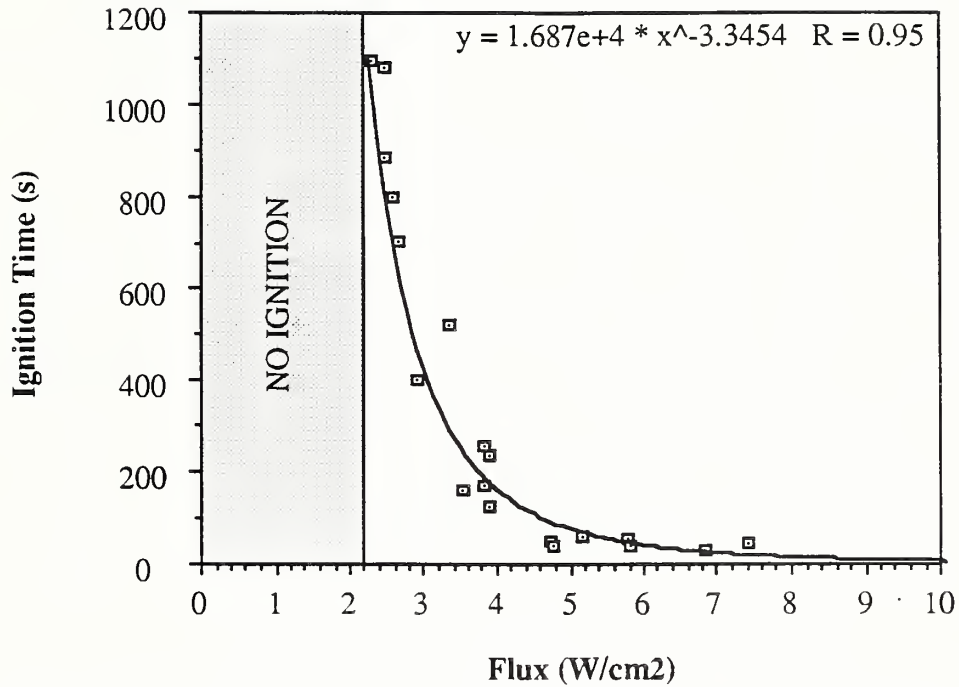


Figure 1 - Ignition delay time vs. incident heat flux for CG Camel honeycomb panel. Equation shown is least-squares fit and R is the correlation coefficient.

### CG Camel & CG Yellow Ignition

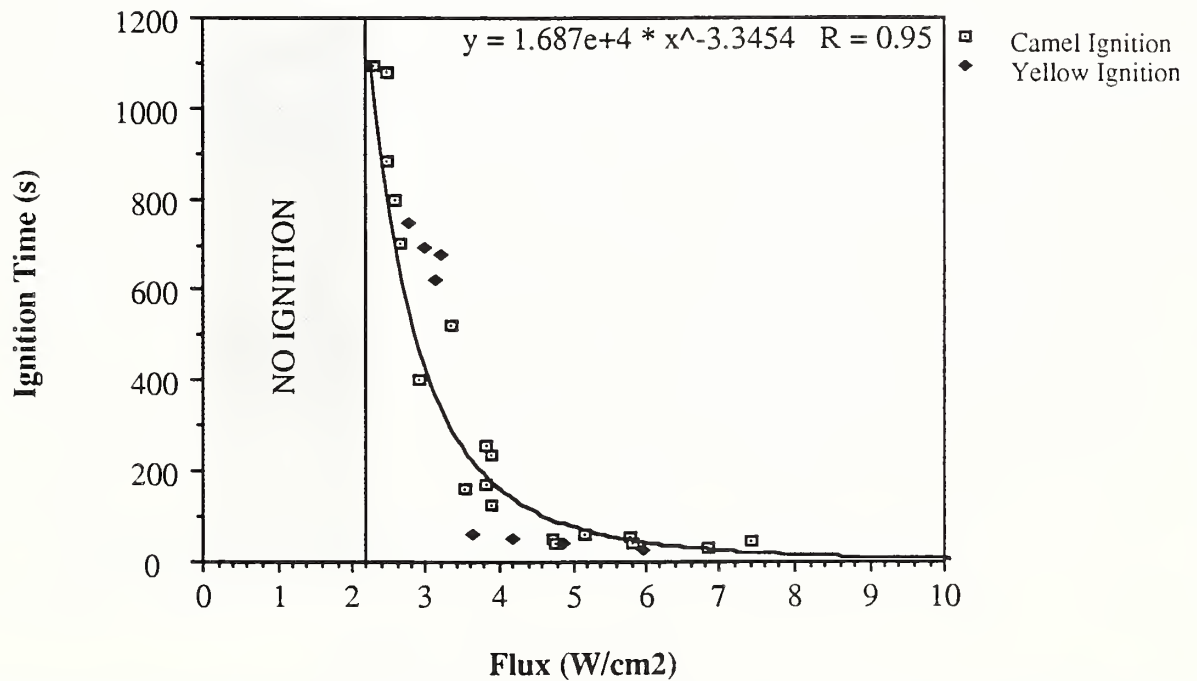


Figure 2 - Ignition delay vs. incident heat flux for CG Camel and CG Yellow honeycomb panels.

### Face vs Edge Ignition of CG Yellow

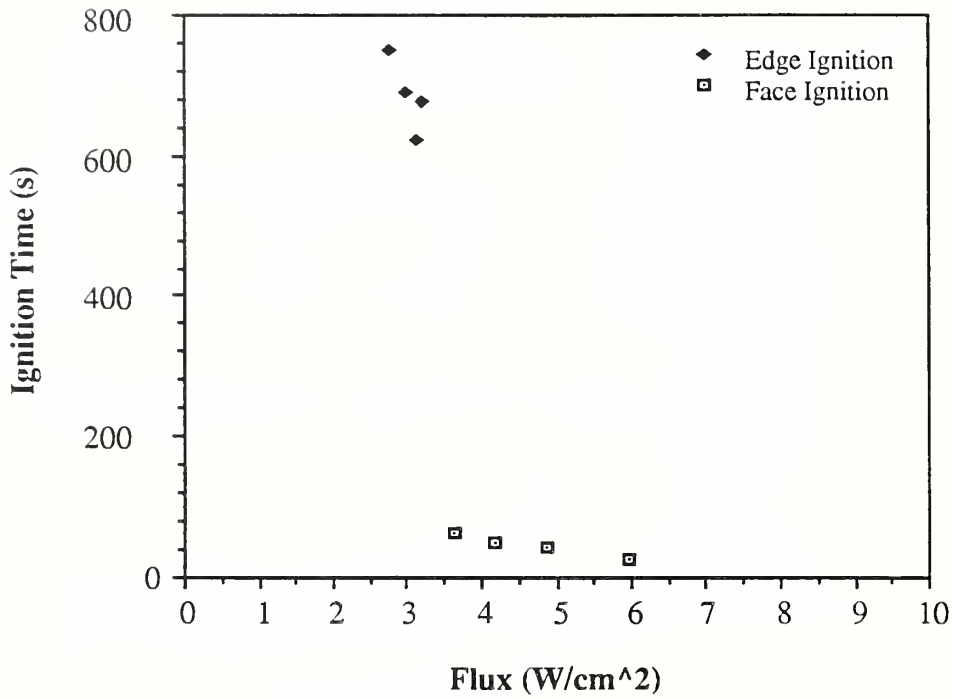


Figure 3 - Ignition delay time vs. incident heat flux for CG Yellow honeycomb panel; face and edge ignition data points are distinguished.

### CG Green Vinyl Ignition

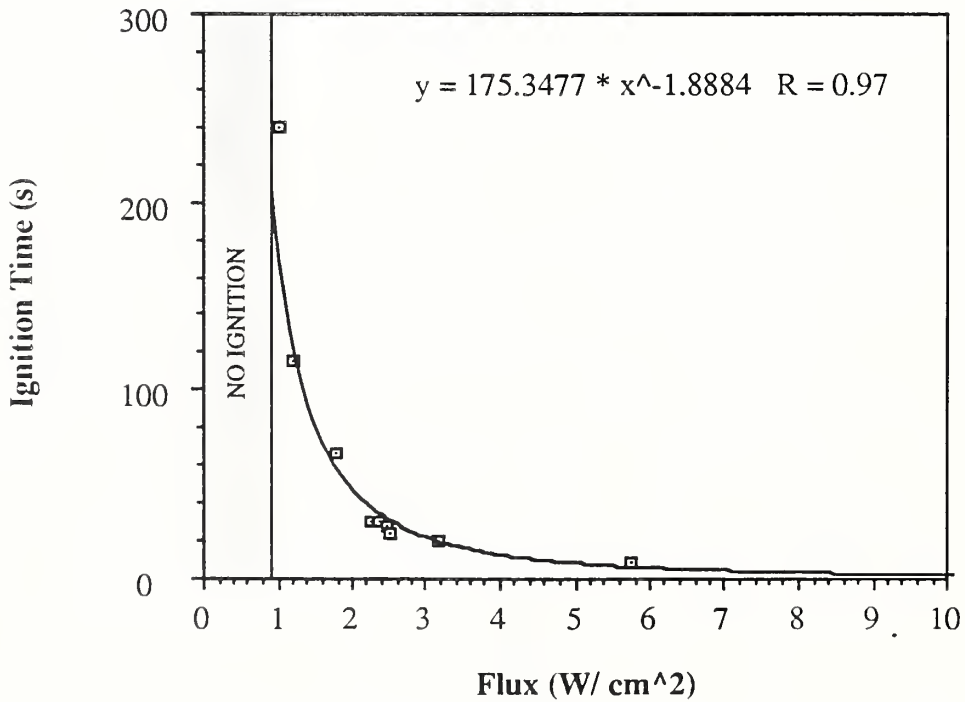
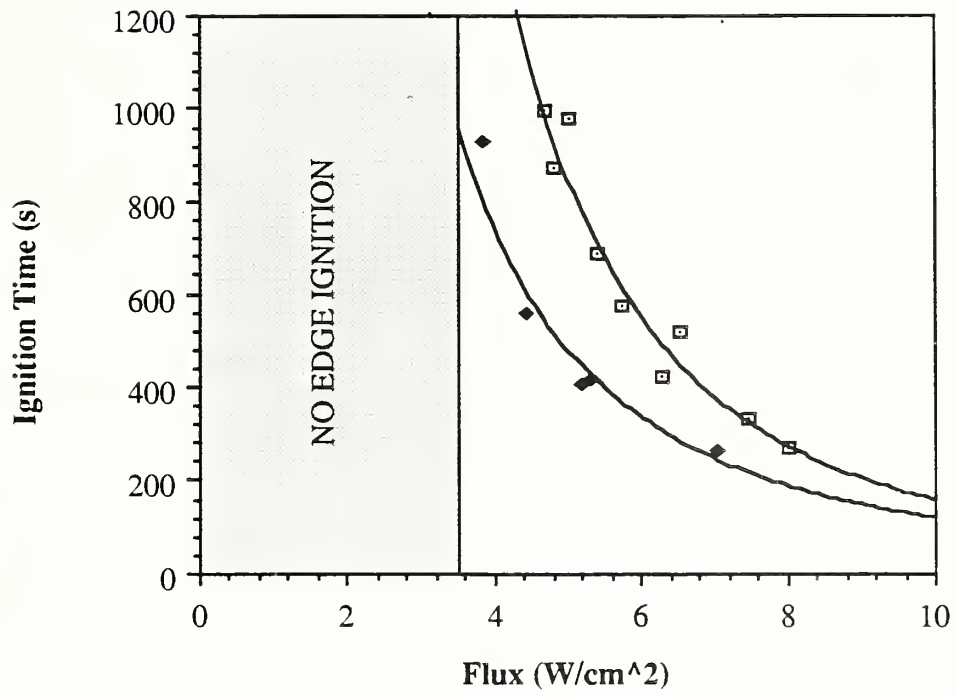


Figure 4 - Ignition delay time vs. incident heat flux for CG Green Vinyl honeycomb panel. Equation shown is least-squares fit and R is the correlation coefficient.

### OC Armor - Face vs Edge - Ignition



$$y = 4.133e+4 * x^{-2.4127} \quad R = 0.98 \quad \square \text{ Face Ignition}$$

$$y = 1.152e+4 * x^{-1.9744} \quad R = 0.98 \quad \blacklozenge \text{ Edge Ignition}$$

Figure 5 - Ignition delay time vs. incident heat flux for OC Armor composite armor panel. Face and edge data points are distinguished. Equations shown are least-squares fits and R values are correlation coefficients.

### CG (Camel & Yellow) Ignition Correlation

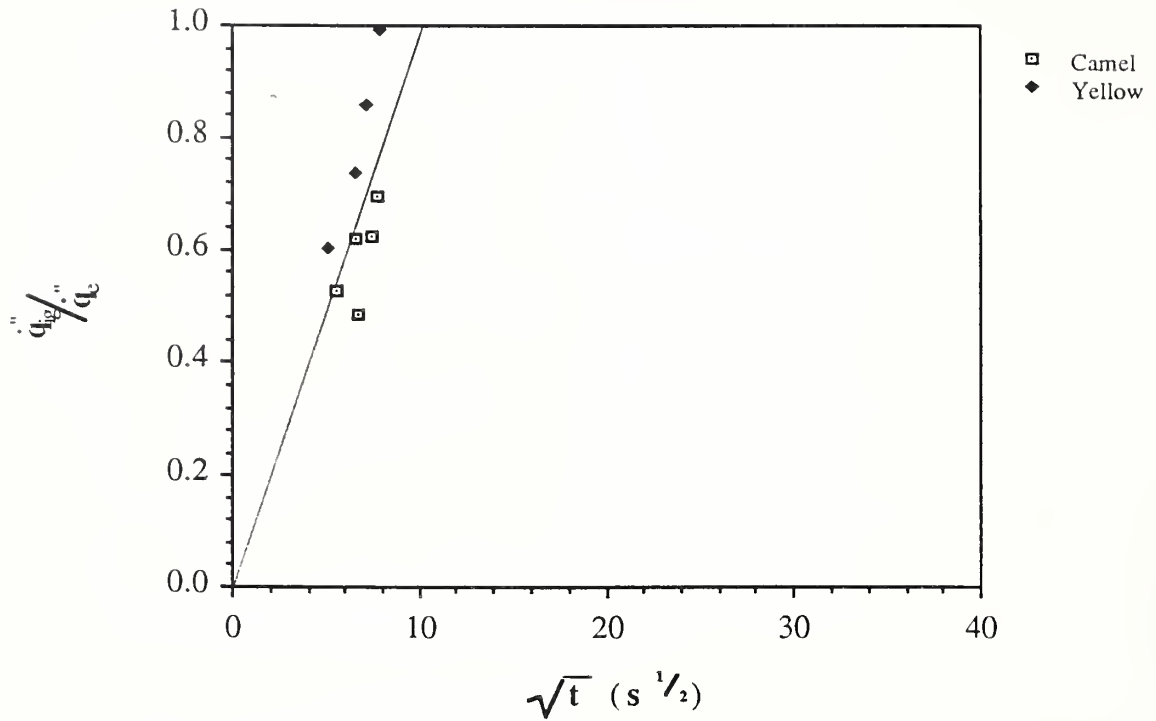


Figure 6 - Ignition model correlation for CG Camel and CG Yellow treated as a single material. Data points for face ignition only.

### CG Green Vinyl Ignition Correlation

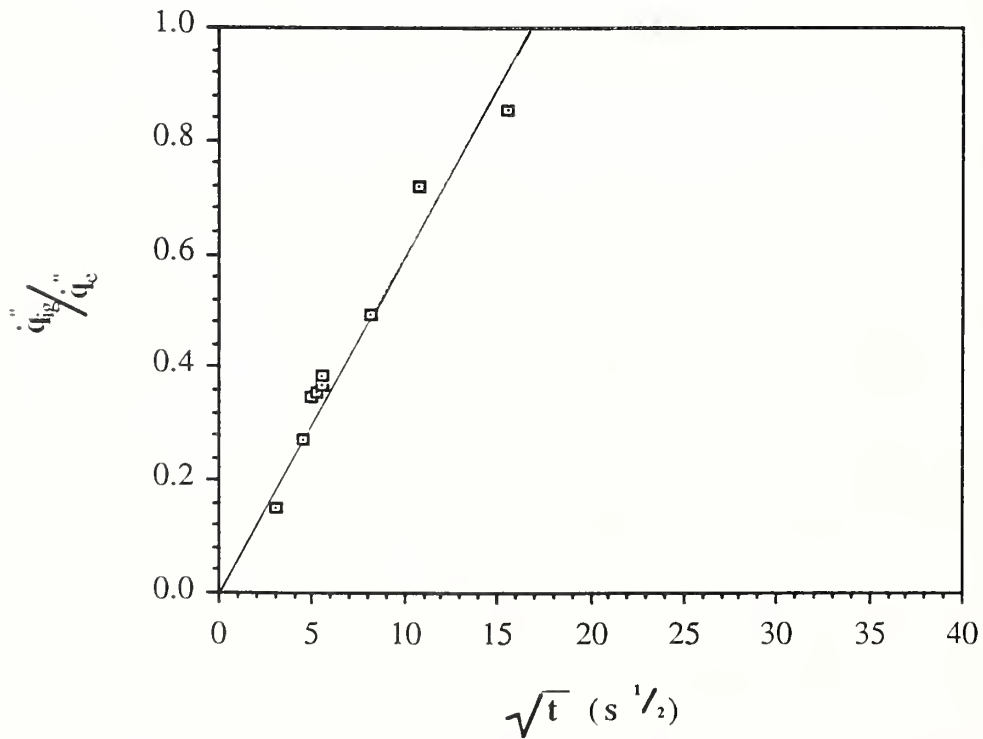


Figure 7 - Ignition model correlation for CG Green Vinyl. Data points for face ignition only.

### OC Armor Face Ignition Correlation

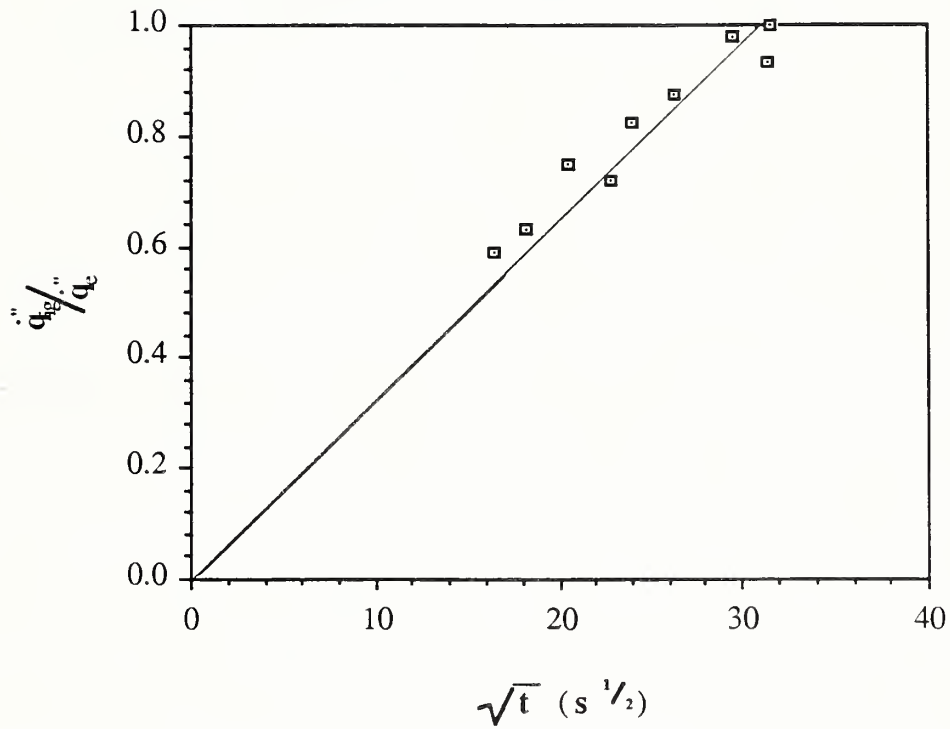


Figure 8 - Ignition model correlation for face ignition of OC Armor.

### OC Armor Edge Ignition Correlation

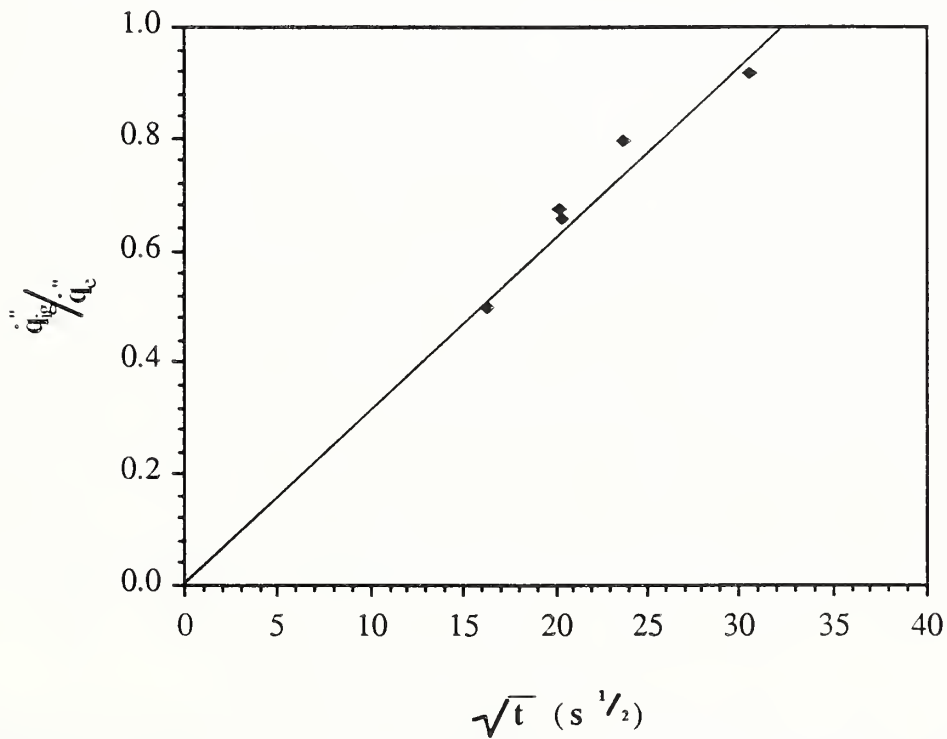


Figure 9 - Ignition model correlation for edge ignition of OC Armor.

### OC Armor Flame Spread

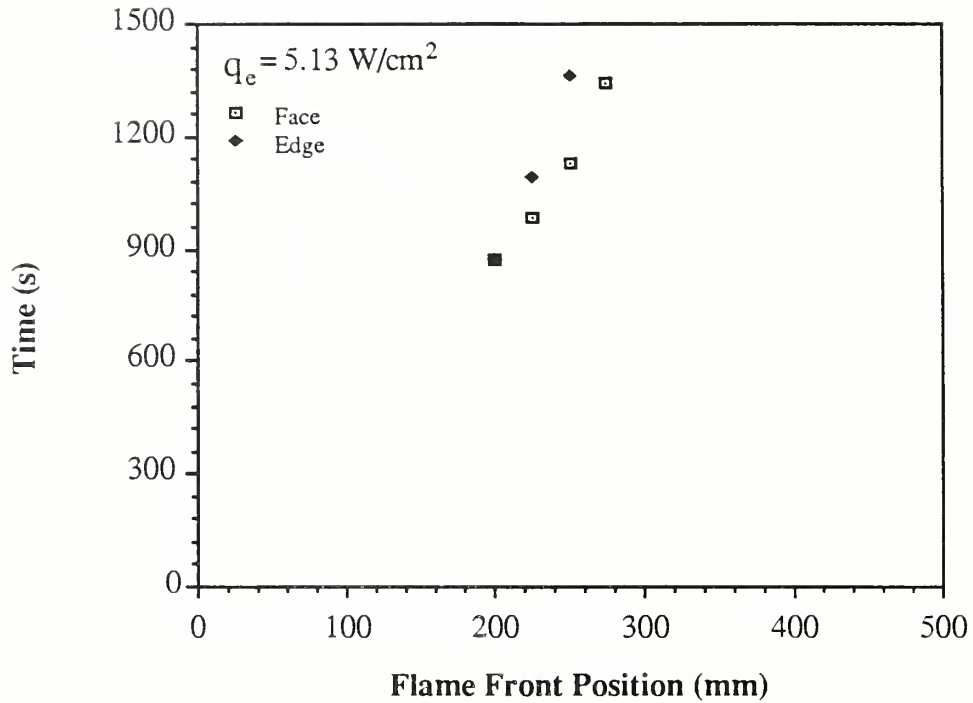


Figure 10 - Experimental data for lateral flame spread on OC Armor. Edge and face data are distinguished. The value of  $q_e$  is the peak incident flux on the sample face.

### CG Camel Flame Spread

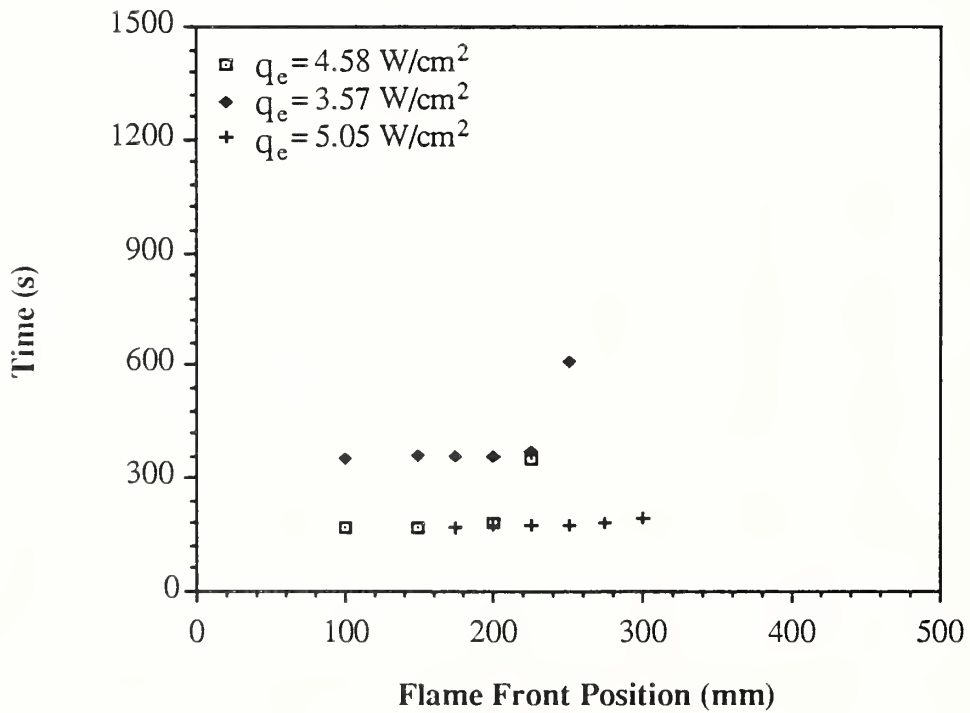


Figure 11 - Experimental data for lateral flame spread on CG Camel honeycomb panel. Data shown are for sample edges. Each test was run at a different value of the peak incident heat flux,  $q_e$ .

### CG Green Vinyl Flame Spread

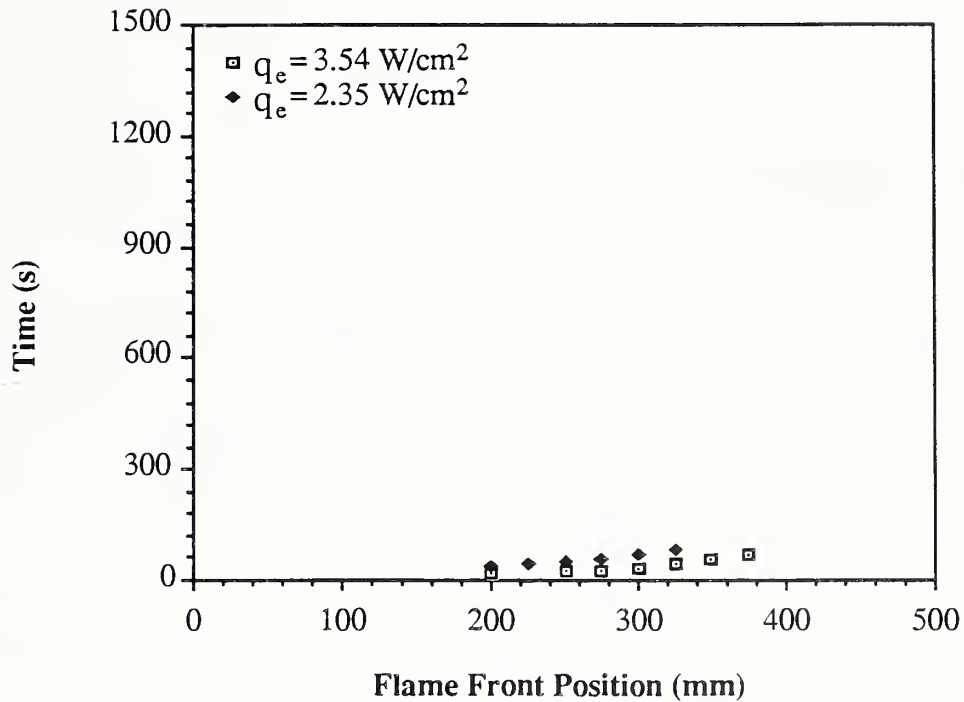


Figure 12 - Experimental data for lateral flame spread on CG Camel honeycomb panel. Data are for sample face. Results for two different values of the peak incident heat flux are shown.

### CG Green Vinyl Flame Spread

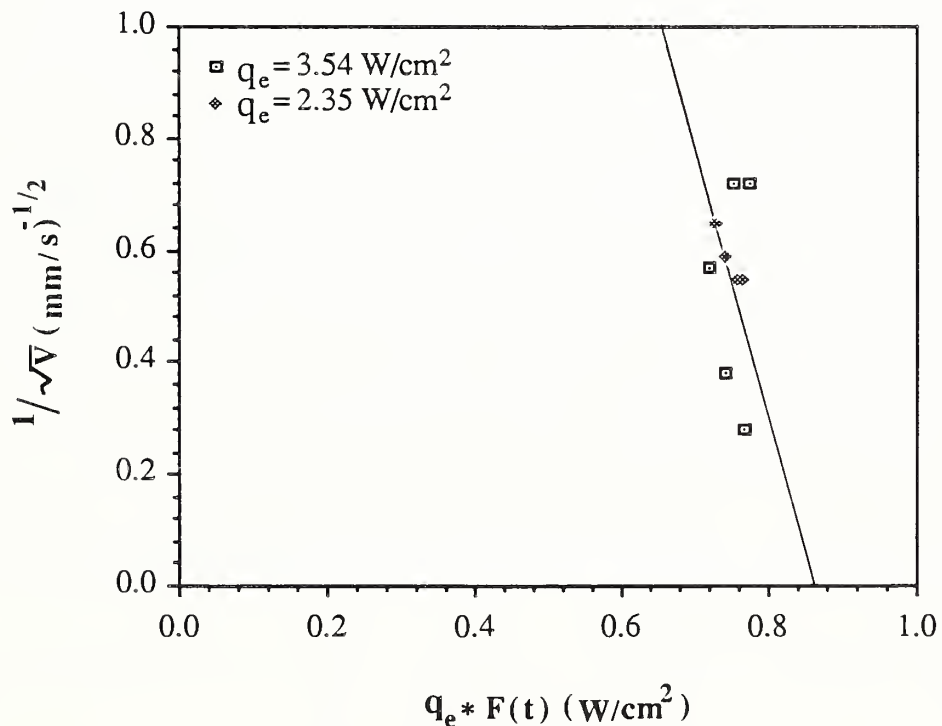


Figure 13 - Model correlation of lateral flame spread on CG Green Vinyl honeycomb panel. Line shown has been forced to pass through a value of 0.87 W/cm<sup>2</sup> on the horizontal axis.

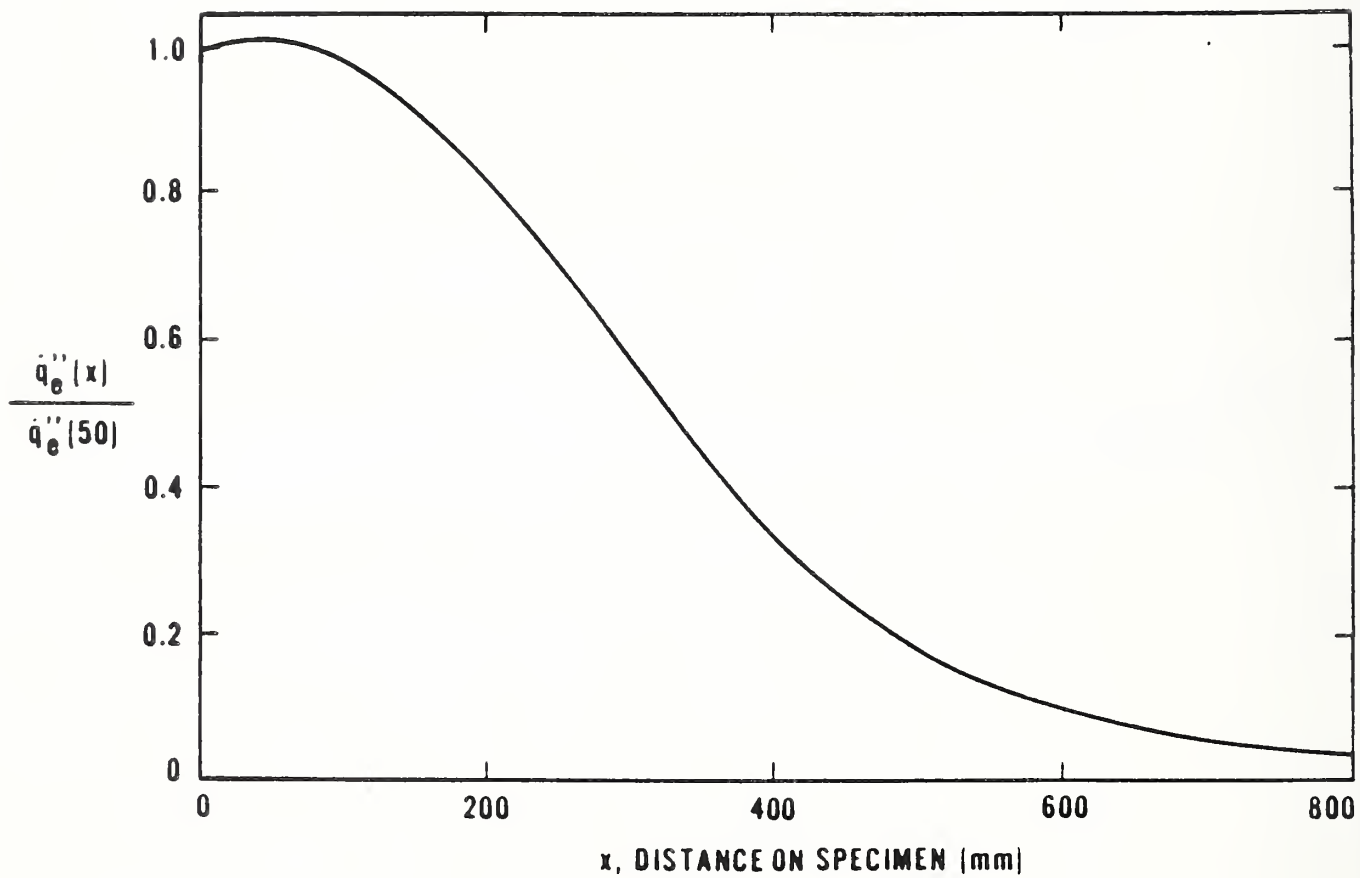


Figure 14 Distribution of heat flux incident on sample surface, normalized by peak value.

U.S. DEPT. OF COMM. <b>BIBLIOGRAPHIC DATA SHEET</b> (See instructions)	<b>1. PUBLICATION OR REPORT NO.</b> NISTIR-89/4030	<b>2. Performing Organ. Report No.</b>	<b>3. Publication Date</b> January 1989
<b>4. TITLE AND SUBTITLE</b> Ignition and Lateral Flame Spread Characteristics of Composite Materials			
<b>5. AUTHOR(S)</b> T. J. Ohlemiller and S. Dolan			
<b>6. PERFORMING ORGANIZATION</b> (If joint or other than NBS, see instructions) National Institute of Standards and Technology U.S. Department of Commerce Gaithersburg, MD 20899			<b>7. Contract/Grant No.</b>
<b>9. SPONSORING ORGANIZATION NAME AND COMPLETE ADDRESS</b> (Street, City, State, ZIP) David Taylor Research Center U.S. Navy Annapolis, MD			<b>8. Type of Report &amp; Period Covered</b>
<b>10. SUPPLEMENTARY NOTES</b>  <input type="checkbox"/> Document describes a computer program; SF-185, FIPS Software Summary, is attached.			
<b>11. ABSTRACT</b> (A 200-word or less factual summary of most significant information. If document includes a significant bibliography or literature survey, mention it here)  <p>The Lateral Ignition and Flame Spread (LIFT) apparatus was used to obtain information on the ignition and lateral flame spread characteristics of two types of composite materials. The first type was a honeycomb sandwich panel; three different facings were tested with this material. The second type of material was a composite armor. There was a substantial variation in the ignitability of the various material combinations with a vinyl-faced honeycomb panel being the most ignitable and the composite armor being the least ignitable. The ignition behavior of the facings of all materials was correlated by a simple predictive model. Only the vinyl-faced honeycomb panel showed significant normal flame spread under the conditions examined though some flame "advancement" was seen with the others. All of the materials exhibited worse flammability properties at their edges as compared to their facings.</p>			
<b>12. KEY WORDS</b> (Six to twelve entries; alphabetical order; capitalize only proper names; and separate key words by semicolons) composite materials; flame spread; flammability; ignition			
<b>13. AVAILABILITY</b>  <input checked="" type="checkbox"/> Unlimited <input type="checkbox"/> For Official Distribution. Do Not Release to NTIS <input type="checkbox"/> Order From Superintendent of Documents, U.S. Government Printing Office, Washington, D.C. 20402.  <input checked="" type="checkbox"/> Order From National Technical Information Service (NTIS), Springfield, VA. 22161			<b>14. NO. OF PRINTED PAGES</b>  29  <b>15. Price</b>  \$11.95





